CHAPTER VI

INFLUENCE OF ELASTICITY ON DISPERSED-PHASE DROPLET SIZE IN IMMISCIBLE POLYMER BLENDS IN SIMPLE SHEARING FLOW

[Wanchai Lerdwijitjarud, Anuvat Sirivat, and Ronald G. Larson,
"Influence of elasticity on dispersed-phase droplet size in
immiscible polymer blends in simple shearing flow",
Polym. Eng. Sci., 42 (4), 798-809 (2002).]

INFLUENCE OF ELASTICITY ON DISPERSED-PHASE DROPLET SIZE IN IMMISCIBLE POLYMER BLENDS IN SIMPLE SHEARING FLOW

ABSTRACT

The influence of elasticity of the blend constituent components on the size and size distribution of dispersed-phase droplets is investigated for blends of polystyrene and high density polyethylene in a simple shearing flow. The elasticities of the blend components are characterized by their first normal stress differences. The role played by the ratio of drop to matrix elasticity at fixed viscosity ratio was examined by using high molecular weight polymer melts, high density polyethylene and polystyrene, at temperatures at which the viscosity ratios roughly equaled each of three different values: 0.5, 1, and 2. The experiments were conducted by using a cone-and-plate rheometer, and the steady-state number and volume-mean averages of droplet diameters were determined by optical microscopy. After steady-state shearing, the viscoelastic drops were larger than the Newtonian drops at the same shearing stress. From the steady-state dispersed-phase droplet diameters, the steady-state capillary number, Ca, defined as the ratio of the viscous shearing stress over the interfacial tension stress was calculated as a function of the ratio of the first normal stress differences in the droplet and matrix phases. For the blend systems with viscosity ratio 0.5, 1 and 2, the values of steady-state capillary number were found to increase with the first normal stress difference ratio and followed a power law with scaling exponents between 1.7 and 1.9.

INTRODUCTION

Although new polymers can be synthesized, they do not always fulfill industrial and technological needs. Moreover, conceiving and synthesizing new polymers involves exorbitant costs and time. Blending is an attractive alternative method of creating new materials with more flexible performance and superior properties than existing polymers (1). Dissolving polymers into each other is thermodynamically unfavorable due to the low entropy of mixing for high molar mass materials. Consequently, many polymer blends are *immiscible*, which gives rise to a multiphase morphology. Generally, when two polymers are mechanically mixed together, the minor phase tends to form spherical drops dispersed in the major matrix phase. The final properties of immiscible polymer blends with spherical morphology are controlled by the size and size distribution of the dispersed phase, which result from drop breakup and coalescence during processing. Therefore, it is expected that a better understanding of the drop breakup and coalescence processes is a necessary condition for a better design and control of a mechanical property of immiscible polymer blends.

Much of the most detailed previous work in the literature on drop breakup and coalescence has focused on Newtonian fluid mixtures. For Newtonian immiscible blends, Taylor's classical theory (2) predicts that for steady-state shearing flows (i.e., for flows in which the shear rate is gradually increased) with negligible inertia, the breakup of an isolated droplet of the dispersed phase is controlled by two dimensionless parameters: i) Capillary number, Ca defined as the ratio between the matrix viscous stress and the interfacial stress and ii) viscosity ratio, η_r defined as the ratio η_d/η_m between dispersed (η_d) and matrix (η_m) phase viscosities. The breakup condition for extensional flows differs from that for shearing flows; for general two dimensional incompressible flows droplet breakup is therefore also controlled by the flow-type parameter α, which is zero for shearing flow and unity for planar extensional flow. Taylor's theory has been extended by Rallison and Acrivos (3), who give detailed predictions of the dependence of critical capillary number, $Ca_{crit} \equiv \dot{\gamma}_c \eta_m D/2\Gamma$ on η_d/η_m and α, where $\dot{\gamma}_c$ is the critical shear rate for breakup.

Experimental studies of isolated Newtonian droplets in Newtonian matrices show good agreement with these predictions (4,5,6,7). The minimum critical capillary number is obtained when the viscosity ratio is around unity.

However, molten polymers are viscoelastic under normal processing conditions, and droplet sizes are expected to be different from those in Newtonian systems due to the influence of elasticity and shear thinning in the matrix and the dispersed phases. The droplet behavior of binary blends when either one phase or the other is viscoelastic has been investigated. Elmendorp and Maalcke (8) studied the contribution of elasticity on the breakup of isolated viscoelastic drops in Newtonian matrices and of Newtonian drops in viscoelastic matrices in a simple shear flow. They found that the more elastic droplets (as measured by the first normal stress difference N_1) were the more stable against breakup, while the more elastic matrices lead to increasingly unstable droplets. Flumerfelt's (9) study of isolated Newtonian droplets in viscoelastic polymer solutions seem to contradict to results of Elmendorp and Maalcke by showing an apparent stabilizing effect of matrix elasticity. However, in Flumerfelt's plots, the viscosity ratio was not held fixed, and this might partly account for differences between the results of Flumerflet and of Elmendorp and Maalcke. Milliken and Leal (10) conducted an experimental investigation of deformation and breakup of isolated viscoelastic drops composed of an aqueous polymer solution in a Newtonian matrix fluid in a planar extensional flow field generated by a four-roll-mill apparatus. They found that, for systems with zero-shear-rate viscosity ratios higher than 0.5, the critical capillary number and the critical deformation (i.e. Taylor's deformation, D, at the critical capillary number) were slightly higher than those of Newtonian drops. However, for systems with zero-shear-rate viscosity ratios less than 0.5, the droplets become unstable to a tip-streaming instability at a low critical capillary number of around 0.15. This unexpected phenomena was further investigated by the same research lab (11, 12). They proposed that the tip-streaming phenomenon in this system is caused by a contamination of an unknown surfactant which possibly is a residue byproduct generated during synthesis of the suspending fluid. Thus the tip streaming is believed to be the result of a Marangoni effect caused by the variation of the surfactant concentration at drop-matrix interface. For the system without surfactant,

the viscoelastic drops deform less than Newtonian drops at a given capillary number and the critical capillary number increases when compared with Newtonian system at an equivalent viscosity ratio.

Blend systems have also been investigated in which both the dispersed phase and matrix phase are viscoelastic. Wu (13) compared the average droplet size of a 15% blend of dispersed phase in an extruded polymer blend with those previously obtained from Newtonian blends. He found that the steady-state capillary number, calculated from the steady-state droplet diameter, of the viscoelastic blend was generally about 10 times larger than that for Newtonian blends at the same viscosity ratio. He also introduced an empirical correlation relating the steady state droplet size of the dispersed phase to the viscosity ratio for several extruded immiscible polymer blend systems. Wu's correlation is $D = 4\Gamma\eta_r^{\pm 0.84}/\dot{\gamma}\eta_m$ where Γ is the interfacial tension between the two components, and $\dot{\gamma}$ is the shear rate. The positive exponent on η_r applies to η_r values greater than unity and the negative exponent to η_r less than unity, so that the minimum D is at $\eta_r = 1$. However, the elasticity of the blends was not included in the correlation, even though the correlation was obtained from viscoelastic materials.

Levitt *et al.* (14) observed drop widening when polypropylene isolated drops were sheared in a high-elasticity polystyrene matrix. They proposed that the width of the flattened drops was dependent upon the difference in storage modulus between matrix and droplet phase. When the viscosity ratio was higher than unity and the ratio of the storage modulus of the droplet phase to that of the matrix phase was larger than two, drop widening was not observed.

Recently, Mighri and co-workers investigated the influence of elasticity contrast, as measured by the ratio, λ_d/λ_m, of the relaxation time of droplet phase, $\lambda_d \equiv N_{1d}/2\eta_d\dot{\gamma}^2$, to that of matrix phase, $\lambda_m \equiv N_{1m}/2\eta_m\dot{\gamma}^2$, on isolated droplet deformation in an elongational flow (15) and on isolated droplet deformation and breakup in a shear flow (16). Here, N_{1d} is the first normal stress difference of the droplet phase and N_{1m} is that of the matrix phase. Constant-viscosity elastic "Boger" fluids were used as model fluids in these studies. They found that the drop deformation diminished as the drop/matrix relaxation-time ratio increased, in either the

elongational or shear flows, which is consistent with the findings of Elmendorp and Maalcke discussed earlier. In shear flow, when $\lambda_d/\lambda_m < 4$, the critical capillary number drastically increased with λ_d/λ_m; but for $\lambda_d/\lambda_m > 4$, it did not change significantly.

Thus, most of the experimental data suggest that elasticity of the droplet phase leads to less deformed, more stable, droplets compared to similar Newtonian droplets, while elasticity of the matrix has the reverse effect. These trends are supported by theoretical considerations, which would suggest that droplet elasticity should augment interfacial tension making droplets less deformable and less breakable. Elasticity of the matrix fluid, on the other hand, should produce high extensional stress near the stagnation point at the downstream end of the droplet leading to tension that tends to stretch the droplet, making it easier to break. Although this simple picture has experimental support, quantitative relationships that link the critical capillary number to droplet or matrix phase elasticity are absent, and some data (such as those of Flumerfelt) seem at odds even with the expected qualitative trends.

Both to aid engineering design of blends, and to spur development of theory, we would like to develop quantitative dimensionless plots of the critical capillary number Ca_{crit} against other dimensionless quantities that characterize melt viscoelasticity, similar to the plots that exist for Newtonian fluids. When both matrix and droplet phases are viscoelastic, Ca_{crit} will depend on the viscosity ratio, and on the dimensionless elasticity of each phase. Since both viscosity and elasticity are shear-rate dependent quantities, and since elasticity is a function of both flow type and flow history, both of which are complex functions of the flow in and around the droplet, no rigorous correlations are likely to be obtainable. Nevertheless, if is at least worth investigating whether meaningful correlations might be obtained using only the most important, most easily measured, quantities. We believe these quantities to be the shear viscosities $\eta_d(\dot{\gamma})$ and $\eta_m(\dot{\gamma})$, and the first normal stress differences $N_{1d}(\dot{\gamma})$ and $N_{1m}(\dot{\gamma})$ of droplet and matrix fluids, all at the shear rate of the flow. The appropriate viscosity of the droplet fluid presumably depends on the strength of the droplet flow field, which becomes weaker for more viscous droplets.

Nevertheless, if the viscosities of the matrix and droplet phases are similar, it might be reasonable, and is certainly simpler, to evaluate all quantities at the imposed shear rate $\dot{\gamma}$ of the macroscopic flow. From these and the other parameters of the problem, we can assemble the following dimensionless groups: $Ca \equiv \dot{\gamma}\eta_m(\dot{\gamma})D/2\Gamma$, $W_{im} \equiv N_{1m}(\dot{\gamma})/(\dot{\gamma}\eta_m(\dot{\gamma}))$, $\eta_r \equiv \eta_d(\dot{\gamma})/\eta_m(\dot{\gamma})$, and $N_{1r} \equiv N_{1d}(\dot{\gamma})/N_{1m}(\dot{\gamma})$. For concentrated blends, Ca will also in general depend on the volume fraction of dispersed phase ϕ, although for small ϕ, we expect that Ca should reach its dilute asymptote, and become independent of ϕ.

The primary aim of this experimental study is to investigate the influence of elasticity contrast, as measured by the ratio of the first normal stress differences, $N_{1r} \equiv N_{1d}(\dot{\gamma})/N_{1m}(\dot{\gamma})$, between the dispersed and the matrix phases, on steady-state droplet size in uncompatibilized immiscible polymer blends in a simple shear flow. Specifically, we wish to determine the correlation between capillary number and the normal stress difference ratio at several fixed values of the viscosity ratio at high values of the Weissenberg number $W_{im} \equiv N_{1m}(\dot{\gamma})/(\dot{\gamma}\eta_m(\dot{\gamma}))$. An attempt will be made to normalize the correlations obtained at various viscosity ratios near unity from different viscoelatic material pairs to see if a unique or common correlation can be obtained. The work presented here is by no means comprehensive. In particular, we will not explore limits in which the droplet or matrix phase becomes weakly, or not at all, elastic. Our hope is that our work will assist in the development of general correlations and predicted theories for estimating droplet sizes in sheared polymer blends.

EXPERIMENTAL

Materials

The materials used in this study are two grades of high-density polyethylene (HDPE), donated by Bangkok Polyethylene, and three grades of polystyrene (PS), purchased from Aldrich and Polysciences, as the matrix and dispersed phases, respectively. The properties of all the polymers are tabulated in Table 4.1. The weight average molecular weights of the polystyrenes were determined by gel permeation chromatography (GPC) (model Waters 150C Plus). The molecular weights of high density polyethylene were obtained by fitting the zero-shear viscosity data with a 3.4-power correlation for 190 °C ($\eta_0 = 5.8 \times 10^{-14} M_w^{3.41}$) reported by Arnett and Thomas (17).

Preparation and Characterization

Characterization of the Rheological Properties of Pure Polymers

The steady-state shear viscosity and the first normal stress difference of each polymer was measured by a cone-and-plate rheometer (Rheometric Scientific, model ARES) (25-mm plate diameter with cone angle 0.1 rad.). The rheological properties were obtained at shear rates between 0.1 and 1 s^{-1} using the rate sweep test mode, and at shear rates higher than 1 s^{-1} using the transient test mode. In the latter mode, both viscosity and first normal stress difference increased rapidly after an initiation of shearing and subsequently reached the steady-state constant values for measurements at low shear rate. Prior to attainment of the steady-state values, the overshoots of η and N_1 were also observed for measurements at high shear rate. For all measurements, the steady-state values were typically obtained within a strain of 15 for the viscosity and 30 for N_1, whereas the strain at the occurrence of edge-fracture decreased with increasing of shear rate. Thus, edge-fracture effects could be minimized by acquiring data after the overshoot but before the onset of significant

edge fracture at each shear rate. Figures 4.1 and 4.2 show the dependences of viscosity and the first normal stress difference on shear rate for all polymers studied at various temperatures.

Polymer Blend System Selection

We define the viscosity ratio, $\eta_r(\dot{\gamma})$, to be the ratio of the viscosity of the dispersed phase at a given shear rate $\dot{\gamma}$ to the matrix phase at that same shear rate $\dot{\gamma}$. Similarly, we define the first normal stress difference ratio, $N_{1r}(\dot{\gamma})$, to be the ratio of the first normal stress difference of the dispersed phase at shear rate $\dot{\gamma}$ to that of the matrix phase at the same shear rate $\dot{\gamma}$. We choose polymer blend systems whose viscosity ratio remains roughly independent of shear rate at the value 0.5 (A systems), 1.0 (B system), and 2.0 (C systems) but the first normal stress difference ratio varies with shear rate under the same testing conditions. The interfacial tension, Γ, between HDPE and PS and the temperature dependence of interfacial tension, $d\Gamma/dT$, were taken from the literature (18). The values of Γ at 150 ^{0}C and $d\Gamma/dT$ are 5.7 mN/m and 0.020 mN/m-K, respectively. Table 4.2 lists the polymer blend systems chosen, the components of the systems, the temperatures, the ranges of shear strain rate covered in the experiments, the viscosity ratios, and the first normal stress difference ratios. Figure 4.3 shows the η_r and N_{1r} values of the studied blend systems.

Polymer Blend Preparation

The composition for all blends studied was 80% by weight HDPE and 20% by weight PS. Before mixing, all polymers were heated to 80 °C under vacuum to eliminate any volatile substances. Constituent component polymer powders of binary blends were weighed, macroscopically mixed and then molded into a disk-like form using a compression molding machine (Wabash, model V50H-18-CX), at the molding temperature of 145 °C.

Melt Blending and Shearing

For each blend system, we determined the shearing time required at a given shear rate to attain a steady-state morphology. The compressed samples were loaded for melt blending and shearing using a Rheometrics mechanical spectrometer (Rheometrics Scientific, model ARES) with a 25-mm. cone-and-plate fixture with a cone-tip truncation of 0.051 mm. The steady-state shearing mode was used. For a given blend system, temperature and shear rate were fixed, and the minimum shearing time was determined as the time after which the mean drop size no longer changed with further shearing. The product of the shearing time and the shear rate gives the strain.

To study the influence of shear rate on the steady-state blend morphology, an initial steady-state morphology was first prepared at either a high or low shear rate. Then, the sample was further sheared at a desired strain rate until a final steady-state average drop size was obtained. After melt blending and subsequent shearing at the desired conditions were complete, the edge of each blend sample was cut away from the sample to remove any portion of the sample influenced by edge fracture from morphology measurement. The blend samples were cooled down to ambient temperature and stored under moisture-free conditions at room temperature for later study.

Morphology Investigations

The samples were cut into 16-30 μm thin films by using a microtome (RME, Model MT 970) with tungsten-carbide cutter and placed onto the microscope glass slides at ambient temperature. Since the glass transition temperature of polystyrene is around 100 °C, the microtome-cutting step did not deform appreciably the PS droplets. An optical microscope (Leica, Model DMRX) with 100x objective lens and 10x eye piece was used to examine the morphology of the chosen blends. Because the microtomed samples were prepared to be quite thin (16-30 μm), light could penetrate and transmit through easily; hence actual drop sizes were seen and

optical correction was not required. The morphological images of immiscible blends were recorded by a CCD camera and data were transferred to a PC computer. Our measuring system had a size resolution of 0.129 μm/pixel. Dispersed-phase droplet size and size distribution were determined by using the image analysis program LEICA Qwin 2.0. Typically 200 drops were required to construct a precise average drop size from each sample. From the droplet size distribution, the number-average diameter, D_n, and the volume-average diameter, D_v, were calculated using the following equations:

$$D_n = \frac{\sum n_i D_i}{\sum n_i} \qquad D_V = \frac{\sum n_i D_i^4}{\sum n_i D_i^3}$$

where n_i is the number of droplets with diameter D_i. The polydispersity of the droplet diameter was calculated as the ratio D_v/D_n.

RESULTS AND DISCUSSION

The Evolution of the Blend Morphology

The effect of shearing time on the blend morphology was investigated. The shear strain, which is the product of the shearing time and the shear rate, was chosen as a variable to indicate the effect of shearing. Figure 4.4 illustrates the dependence of D_n, D_v, and D_v/D_n on strain for the blend system A1 (Table 4.2) at the shear strain rate of 30 s^{-1}. The optical micrographs of this blend at different strains are depicted in Figure 4.5.

As can be seen in Figures 4.4 and 4.5, at low shear strain, the droplet size distribution is wide and correspondingly the polydispersity of droplet size is quite large. As the shear strain increases, the droplet size distribution becomes narrower and a smaller dispersity index is obtained. At strains greater than 2,000-3,000 , D_n, D_v and D_v/D_n cease to change much. The same procedure was applied for all blend systems studied and similar results were achieved. Thus, 3,000 strain units are chosen as a minimum for obtaining steady-state droplet sizes for all blends. This value is consistent with the experimental results of Lyu *et al.* (19) who studied coalescence of PS/HDPE blends in shearing flow generated by a cup-and-cone geometry. They found that for the blend systems with $\eta_r = 1.05$ and volume fractions of HDPE equal to 12.7% and 24.6%, D_v did not significantly change after the strain reached 1,000 units for all shear rates studied, i.e., 0.1, 1, and 2.5 s^{-1}. It was also found that a strain of 2,000–3,000 was adequate to attain a steady-state morphology for other blends (20, 21).

The Effect of Shear Rate on the steady-State Blend Morphology

The effect of shear rate on the steady-state blend morphology of blend system A2 is shown in Figure 4.6. The filled symbols in Figure 4.6 were each obtained by preparing an initial sample morphology at the shear strain rate 5 s^{-1}, followed by a step up in shear rate to 7, 10, 20 and 30 s^{-1}. The open symbols in Figure 6 were obtained from an initial sample morphology at a high shear rate, 30 s^{-1}, and

subsequently stepping down the strain rate to 20, 10, 7 and 5 s^{-1}. The steady-state morphology shown was evidently controlled by the dynamic equilibrium between drop breakup and drop coalescence under the shearing process. Drop breakup dominates after the shear rate is stepped up, leading to smaller droplet size. On the other hand, drop coalescence is more pronounced after the shear rate of the system is stepped down. The filled and unfilled symbols coincide almost perfectly; in fact, the filled symbols are almost completely covered by the open symbols for some shear rates. Thus, hysteresis was not observed in blend system A2 at shear strain rates between 5 and 30 s^{-1}.

The steady-state number-average droplet diameter (D_n), volume-average droplet diameter (D_v) and polydispersity of droplet diameters (D_v/D_n) for all blend systems studied are summarized and tabulated in Table 4.3. The dependences of D_n on the shear rate of the blend systems A1 and A2 are shown in Figure 4.7a. As predicted by Talor's theory, the steady state droplet sizes have been found to be approximately inversely proportional to the applied shear rate for Newtonian-fluid blend system (20,21,22). In contrast to a Newtonian drop in a Newtonian matrix system, where $D \propto \dot{\gamma}^{-1}$, we find that the sizes of our viscoelastic drops in viscoelastic matrices depend on shear rate as follows: i) $D_n \propto \dot{\gamma}^{-0.16}$ and $D_v \propto \dot{\gamma}^{-0.17}$ for blend A1, and ii) $D_n \propto \dot{\gamma}^{-0.19}$ and $D_v \propto \dot{\gamma}^{-0.22}$ for blend A2. The small scaling exponents suggest that the viscoelastic drops are progressively more difficult to break relative to Newtonian drops at increased shear rate due to the increasing elasticity of the drop, and because the increase in viscous force for a given increase in shear rate is less for shear-thinning polymer melts than for Newtonian fluids. To eliminate the contribution of shear-thinning effect of matrix, a correlation between D_n and D_v on $\dot{\gamma}\eta_m(\dot{\gamma})/\Gamma$ was constructed (Figure 4.7b), where the matrix viscosity $\eta_m(\dot{\gamma})$ was evaluated at the shear rate at which the droplet size was measured. Despite accounting for shear thinning in this way, the dependence of steady-state droplet size of viscoelastic drops on $\dot{\gamma}\eta_m(\dot{\gamma})/\Gamma$ remains weaker than that of a Newtonian drop in a Newtonian matrix system as shown by the power-law exponents, i.e. for blend A1: $D_n \propto (\dot{\gamma}\eta_m(\dot{\gamma})/\Gamma)^{-0.25}$, $D_v \propto (\dot{\gamma}\eta_m(\dot{\gamma})/\Gamma)^{-0.26}$ and for blend system A2: $D_n \propto (\dot{\gamma}\eta_m(\dot{\gamma})/\Gamma)^{-0.28}$, $D_v \propto (\dot{\gamma}\eta_m(\dot{\gamma})/\Gamma)^{-0.31}$. This seems to confirm that a

viscoelastic drop is increasingly more difficult to break compared to a Newtonian drop at increasing shear rates.

The Effect of the First Normal Stress Difference Ratio on the Steady-State Blend Morphology

From the steady-state volume-average droplet diameter, D_v, of the dispersed phase, the steady-state capillary number, Ca, defined as the ratio of the viscous shearing force, $\dot{\gamma}\eta_m(\dot{\gamma})$, to the interfacial stress, $2\Gamma/D_v$, calculated from the steady-state droplet size, D_v, was determined. The resulting steady-state capillary numbers were plotted versus the first normal stress difference ratios of the blend systems in Figure 4.8. For the blend systems studied having viscosity ratios of 0.5, 1 and 2, the steady-state capillary numbers calculated from D_v are found to increase with the first normal stress difference ratio, N_{1r}, and follow a power law with scaling exponent near 2.0.

Our results are consistent with both theoretical expectations and most previous literature in showing that the critical capillary number increases with increasing droplet elasticity and with decreasing matrix elasticity. We have also found the rather surprising result that Ca seems to correlate well with N_{1r}, first normal stress difference ratio of droplet to matrix phases. This result is certainly not generally valid since if both phases are made less elastic at fixed N_{1r}, the critical capillary number must approach the same Newtonian value, no matter what the ratio of normal stress difference N_{1r} happens to be in this limit. An interesting topic for future research will be to investigate how Ca approaches its Newtonian value when both phases are made progressively less elastic.

It should be noted that the shear rate inside the droplet is in general different from the imposed shear rate. Depending on the viscosity ratio, the shear rate inside the droplet will either be higher or lower than the applied shear rate. In addition, the shear rate inside the droplet is not uniform and also depends on the shape of deformed drop. Typically the shear rate inside the ellipsoidally deformed droplet is highest at droplet-matrix interface and progressively decreases as one moves towards the major axis of deformed droplet due to the circulation of droplet fluid. Thus, the

N_1 value inside the droplet will not be uniform and will be a complex function of shear rate, viscosity ratio, and droplet shape. Here, for simplicity, we used the nominal N_1 value at the imposed shear rate as an index of the magnitude of the normal stress effects. While this does not capture the influence of N_1 quantitatively, it should at least reveal the trend in the dependence of N_1 on the droplet size, as long as the viscosity ratio is held fixed.

It is surprising how sensitive our results are to the viscosity ratio $\eta_r \equiv \eta_d(\dot{\gamma})/\eta_m(\dot{\gamma})$. On figure 8, the lines for $\eta_r = 0.5$ and 1 are separated from each other by a factor of two along the N_{1r} axis, while the lines for $\eta_r = 1$ and 2 are separated by a factor of four. The sensitivity to η_r can perhaps be explained by noting that as the droplet phase becomes relatively more viscous, the flow field in the droplet will become weaker. Since the droplet-phase normal stress difference N_{1d} is very sensitive to shear rate (see Figure 4.2b), normal stresses actually generated in the viscous droplet will be much less than the nominal value used in the abscissa of figure 4.8. In fact, since $N_{1d}(\gamma)$ follows a rough power law in $\dot{\gamma}$ with exponent in the range 1-2, one might expect a 2-to-4-fold smaller N_{1d} value in the droplet to result from a doubling of the droplet viscosity at fixed matrix viscosity, for viscosity ratios of unity or greater. At low viscosity ratios $\eta_r << 1$, the flow in the droplet should become less sensitive to η_r and we should expect a weaker synergy between the effects of η_r and N_{1r}. The data of figure 8 are consistent with this expectation, but data at η_r values less than 0.5 will be required to confirm it.

CONCLUSIONS

We have investigated the contribution of contrast in elasticity between the droplet and matrix phase on dispersed-phase droplet size for blends of high density polyethylene and polystyrene with viscosity ratio 0.5, 1 and 2. The elasticity contrast is measured by ratio, $N_{1r} \equiv N_{1d}/N_{1m}$, of the first normal stress difference of dispersed (N_{1d}) to that of matrix (N_{1m}) phase. The viscoelastic drops in a viscoelastic matrix are more difficult to break compared to Newtonian drops in a Newtonian matrix, due to the contribution of both droplet elasticity and shear-thinning of the polymer matrix. For all blend systems studied, the steady-state capillary numbers (i.e., dimensionless droplet sizes) were found to increase with N_{1r} and are correlated by a power law in N_{1r} with scaling exponents in the range 1.7 – 1.9.

ACKNOWLEDGEMENTS

The authors wish to acknowledge the fellowships provided by Thailand Research Fund (TRF) in the Royal Golden Jubilee Ph D. Program grant no. PHD/00144/2541 and TRF-BRG grant no. BRG/12/2544.

REFERENCES

U. Sundararaj, and C. W. Macosko, *Macromolecules*, **28,** 2647 (1995).

G. I. Taylor, *Proc. R. Soc.*, **A138**, 501 (1934).

J. M. Rallison, and A. Acrivos, *J. Fluid Mech.*, **89**, 191 (1978).

H. P. Grace, *Chem. Eng. Commun.*, **14**, 225 (1982).

B. J. Bentley, and L. G. Leal, *J. Fluid Mech.*, **167**, 241 (1986).

R. A. de-Bruijn, *Deformation and Breakup of Drops in Simple Shear Flow*, Ph.D.Thesis, TU Eindhoven (1989).

J. M. H. Jansen, *Dynamics of Liquid-Liquid Mixing*, Ph. D. Thesis, TU Eindhoven (1993).

J. J. Elmendrop, and R. J. Maalcke, *Polm. Eng. Sci.*, **25**, 1041 (1985).

R. W. Flumerfelt, *Ind. Eng. Chem. Fundam.*, **11**, 312 (1972).

W. J. Milliken, and L. G. Leal, *J. Non-Newtonian Fluid Mech.*, **40**, 355 (1991).

W. J. Milliken, H. A. Stone, and L. G. Leal, *Phys. Fluids*, **5**, 69 (1993).

D. C. Tretheway, and L. G. Leal, *AlChE.*, **45**, 929 (1999).

S. Wu, *Polym. Eng. Sci.*, **27**, 335 (1987).

L. Levitt, C. W. Macosko, and S.D. Pearson, *Polym. Eng. Sci.*, **36**, 1647 (1996).

F. Mighri, P. J. Carreau, and A. Ajji, *J. Rheol.*, **41**, 1183 (1997).

F. Mighri, P. J. Carreau, and A. Ajji, *J. Rheol.*, **42**, 1477 (1998).

R. L. Arnett and C. P. Thomas, *J. Phys. Chem.*, **84**, 649 (1980).

J. Brandrup and E. H. Immergut, *Polymer Handbook*, 3rd ed., New York (1989), p. IV/427.

S. Lyu, F. S. Bates, and C. W. Macosko, *AlChE.*, **46**, 229 (2000).

I. Vinckier, P. Moldenaers, and J. Mewis, *J. Rheol.*, **40**, 613 (1996).

A. J. Ramic, J. C. Stehlin, S. D. Hudson, A. M. Jamieson, and I Manas-Zloczower, *Macromolecules*, **33**, 371 (2000).

S. Kitade, A. Ichikawa, N. Imura, Y. Takahashi, and I. Noda, *J. Rheol.*, **41**, 1039 (1997).

TABLES

Table 4.1 Properties of polymers used.

Polymer	Supplier	Grade	M_w	Melt Flow Index (g/10min)
PS 1	Aldrich	Cat # 43011-0	162,000*	14[+]
PS 2	Polyscience	Cat # 18544	61,000*	-
PS 3	Polyscience	Cat # 23637	67,000*	-
HDPE 1	Bangkok Polyethylene	2208J	72,000**	10[++]
HDPE 2	Bangkok Polyethylene	1600J	68,000**	14[++]

* Measured by gel permeation chromatography based on polystyrene standard calibration.

** Obtained from fitting zero-shear viscosity data with a 3.4-power correlation for 190 °C ($\eta_0 = 5.8 \times 10^{-14} M_w^{3.41}$) reported by Arnett and Thomas (17)

[+] Reported by manufacturers at conditions of 200 ^{0}C, 5.00 Kg. g/10 min , ASTM D1238.

[++] Reported by manufacturers at conditions of 190 ^{0}C, 2.16 Kg. g/10 min , ASTM D1238.

Table 4.2 The polymer blend systems.

Blend system	Blend components	Temperature (°C)	Shear strain rate (s^{-1})	η_r	N_{1r}
A1	80% HDPE1 : 20% PS1 (0.1% Irganox)	220	7 – 70	0.85 – 1.00	0.50 – 0.91
A2	80% HDPE2 : 20% PS2	145	5 – 30	0.83 – 0.99	1.16 – 1.60
B1	80% HDPE2 : 20% PS2	155	3 – 50	0.52 – 0.56	0.36 – 0.77
C1	80% HDPE2 : 20% PS3	143	3 – 7	1.81 – 2.13	3.73 – 4.07
C2	80% HDPE2 : 20% PS3	145	2 – 3	1.89 – 1.98	3.08 – 3.21

Table 4.3 D_n, D_v, and D_v/D_n for blend systems A1, B1, C1, and C2 in a step-up shear-rate experiment and for blend system A2 in both a step-up and step-down shear-rate experiments.

Blend System; Droplet Diameter	Shear Strain Rate (s^{-1})								
	2	3	5	7	10	20	30	50	70
A1[a]; D_n (μm)				2.492	2.291	1.937	1.890	1.758	1.673
D_v (μm)				3.349	3.498	2.655	2.721	2.560	2.233
D_v/D_n				1.344	1.527	1.370	1.439	1.457	1.335
A2[a]; D_n (μm)			9.213	8.533	7.904	7.297	6.229		
D_v (μm)			14.461	12.286	10.978	10.626	9.093		
D_v/D_n			1.570	1.440	1.389	1.456	1.460		
A2[b]; D_n (μm)			9.282	8.407	7.960	7.224	6.283		
D_v (μm)			14.070	12.325	11.749	10.515	9.408		
D_v/D_n			1.516	1.466	1.476	1.456	1.497		
B1[a]; D_n (μm)		7.092	6.951	5.338	4.705	3.583	3.365		
D_v (μm)		10.086	9.966	7.958	6.825	5.259	4.666		
D_v/D_n		1.422	1.434	1.491	1.450	1.468	1.387		
C1[a]; D_n (μm)		8.182	8.029	7.442					
D_v (μm)		15.514	13.314	12.843					
D_v/D_n		1.896	1.658	1.726					
C2[a]; D_n (μm)	8.933	8.272							
D_v (μm)	17.961	15.404							
D_v/D_n	2.011	1.862							

[a] step-up shear-rate experiment

[b] step-down shear-rate experiment

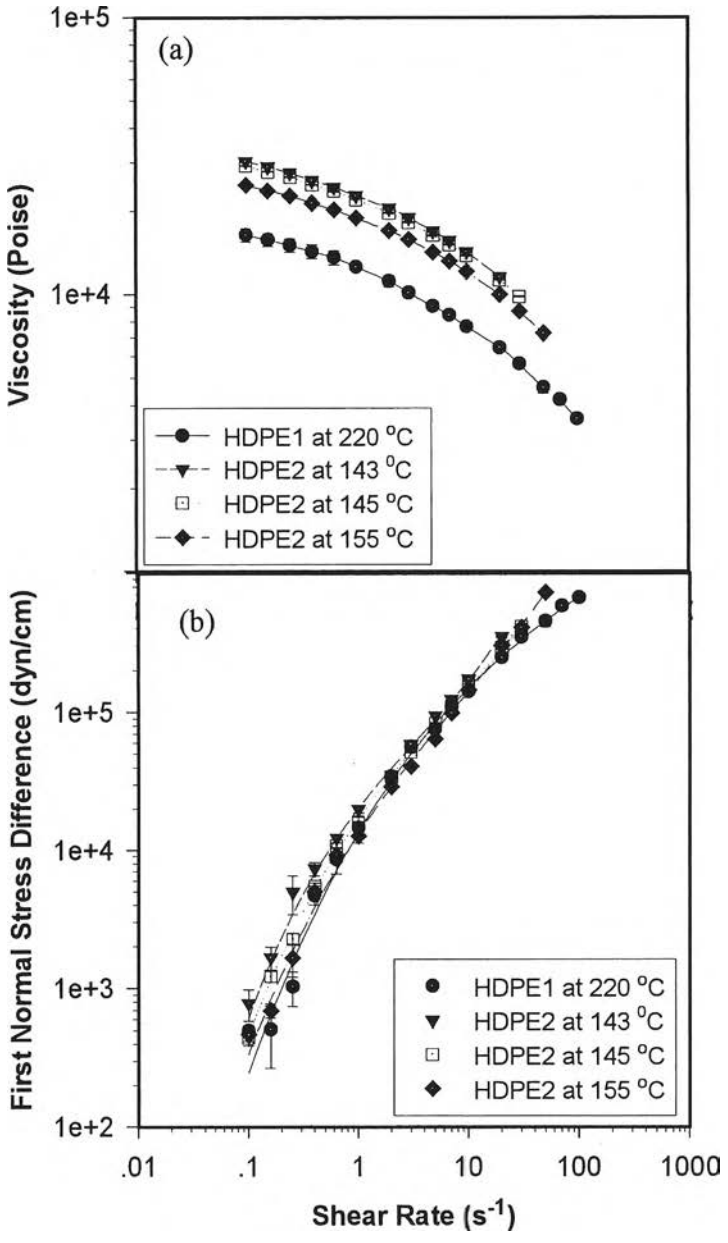

Figure 4.1 The dependence of (a) viscosity and (b) first normal stress difference ratio on shear rate of high density polyethylenes at various temperatures

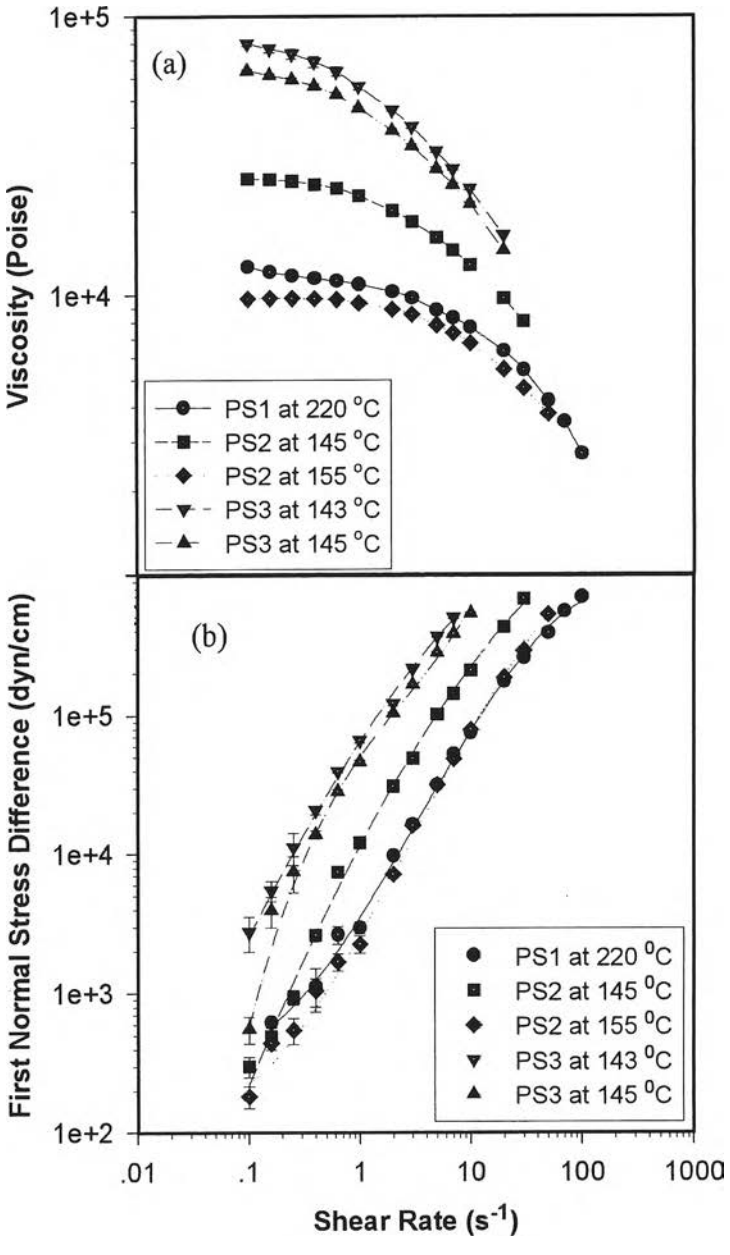

Figure 4.2 The dependence of (a) viscosity and (b) first normal stress difference on shear rate for polystyrenes at various temperatures

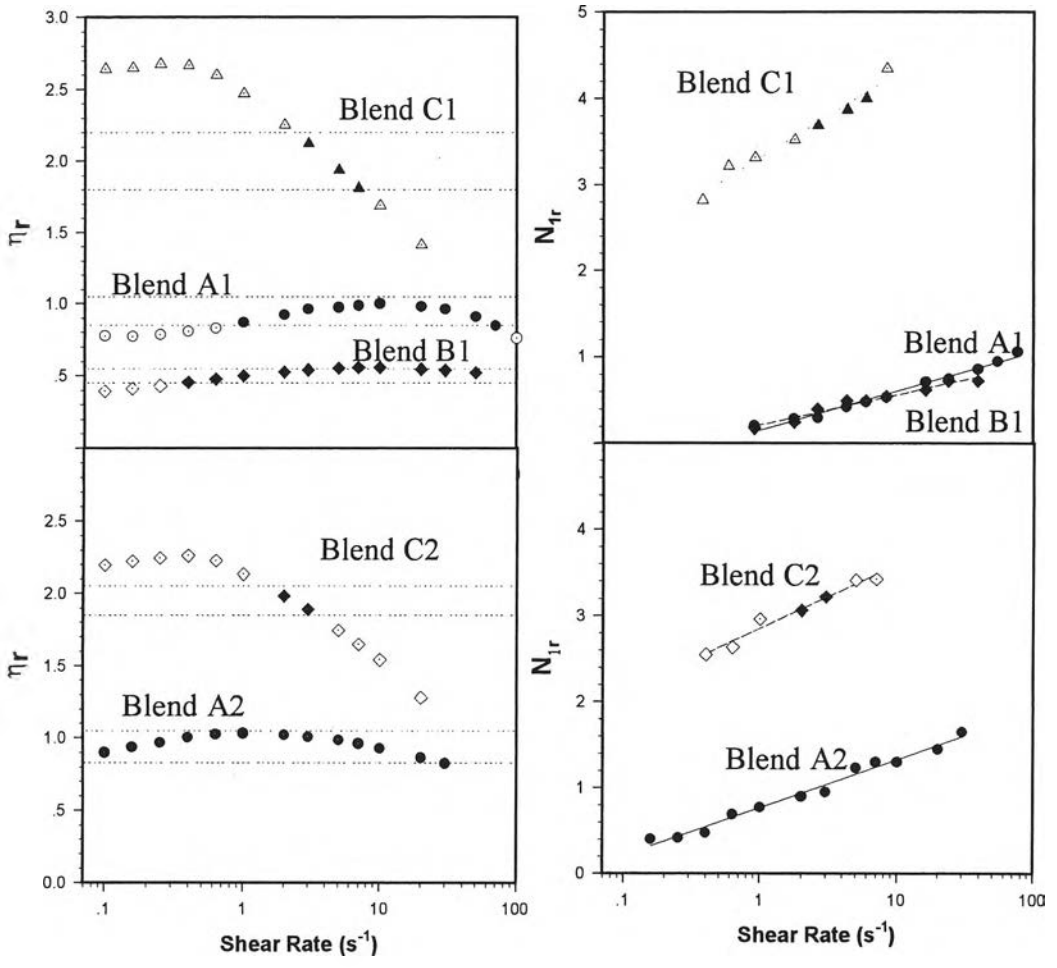

Figure 4.3 The viscosity ratio and the first normal stress difference ratio for all blend systems studied. The horizontal dashed lines and the filled symbols show the ranges of data selected to be sufficiently close to the desired conditions of η_r = 0.5, 1, and 2 for the A, B, and C systems, respectively

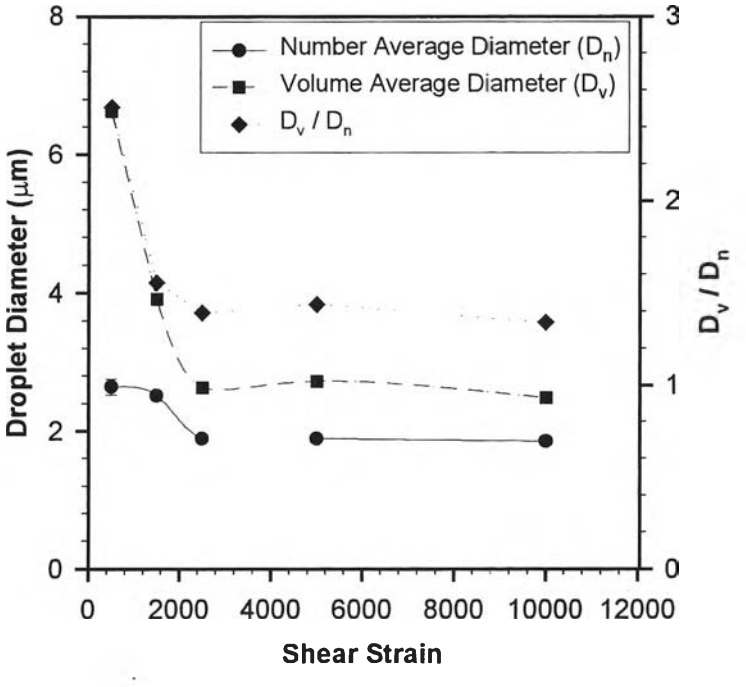

Figure 4.4 The dependence of D_n, D_v, and D_v/D_n on shear strain for blend system A1 at shear rate 30 s^{-1} and temperature 220 °C

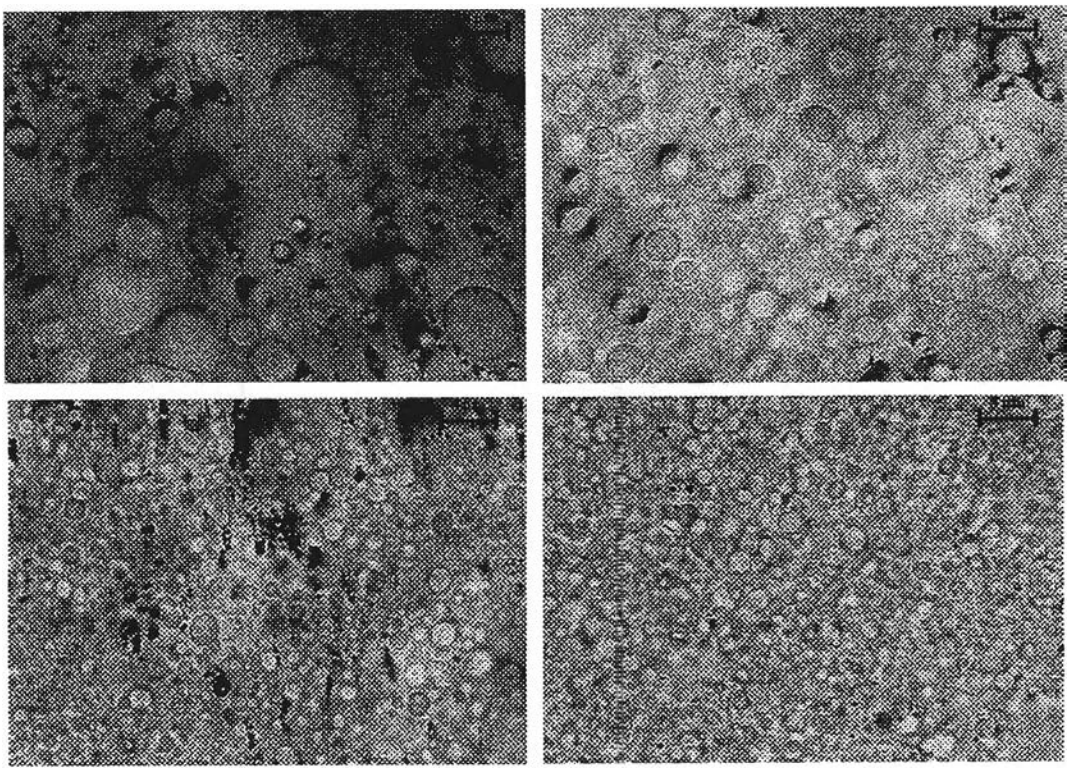

Figure 4.5 Optical micrographs of blend system A1 sheared at 30 s^{-1} for strain of (a) 500 units, (b) 1,500 units, (c) 2,500 units, and (d) 10,000 units. A bar length shown in each image is 8 μm

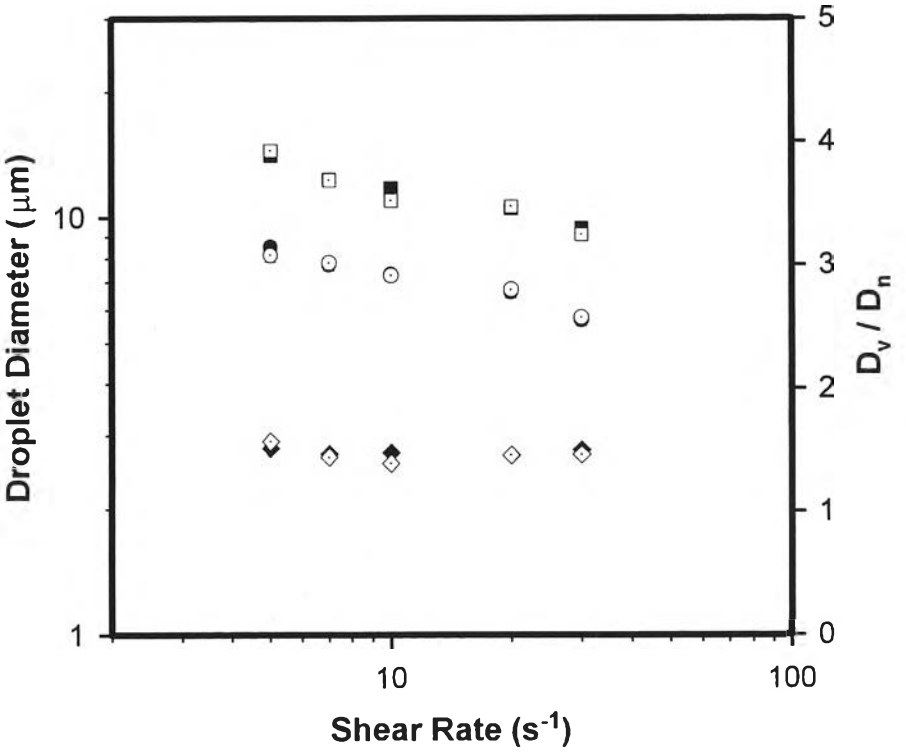

Figure 4.6 D_n, D_v, and D_v/D_n as functions of shear rate for a step up of shear rate from 5 s^{-1} (filled symbols), a step down of shear rate from 30 s^{-1} (open symbols). In many cases, the filled symbols are almost completely covered by the open symbols, showing that results obtained by either increasing or decreasing the shear rate are equivalent

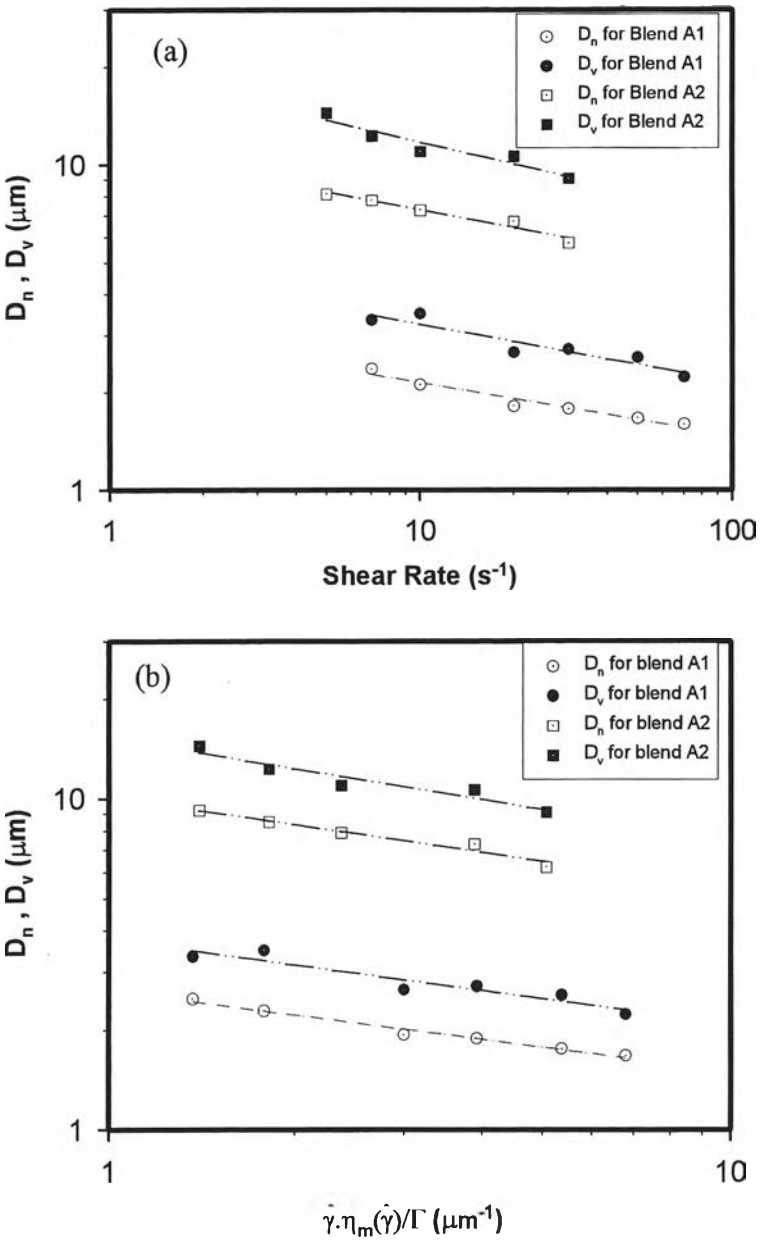

Figure 4.7 (a) The dependence of the steady-state number-average droplet diameter, D_n, and volume-average droplet diameter, D_v, on shear rate for the blend systems A1 and A2. The lines represent power laws with exponents of -0.16, -0.18 for D_n, D_v in blend system A1, and -0.19, -0.22 for D_n, D_v in blend system A2, respectively. (b) The dependence of the steady-state number-average droplet diameter, D_n, and volume-average droplet diameter, D_v, on $\dot{\gamma}.\eta_m(\dot{\gamma})/\Gamma$ for the blend systems A1 and A2. The lines represent power laws with exponents of -0.25, -0.26 for D_n, D_v in blend system A1, and -0.28, -0.31 for D_n, D_v in blend system A2.

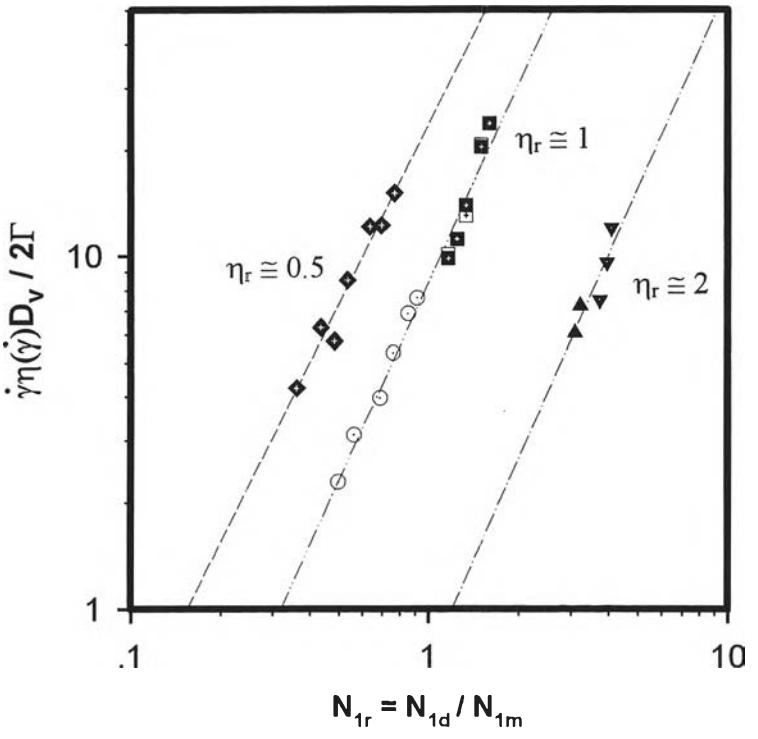

Figure 4.8 The dependences of steady-state capillary numbers calculated from D_v on the first normal stress difference ratios for the blend systems A1 (○) and A2 (□ step down shear rate, ■ step up shear rate) with viscosity ratios $\eta_r \cong 1$, for blend system B1 (◆)with $\eta_r \cong 0.5$, and for blend systems C1 (▼)and C2 (▲) with $\eta_r \cong 2$. The lines describe power laws with exponents of 1.7, 1.9, and 1.9 for $\eta_r \cong 0.5$, 1.0, and 2.0, respectively